SIZE REDUCED COMPOSITE REPAIRS BY PLY WISE SCARFING

D. Holzhüter[1], J. Kosmannn[1], C. Hühne[1,2], M. Sinapius[2,1], M. Schollerer[1]

[1]Institute of Composite Structures and Adaptive Systems, Department of Composite Design, German Aerospace Center, Lilienthalplatz 7, 38108 Braunschweig, Germany
Email: dirk.holzhueter@dlr.de, Web Page: http://www.dlr.de
[2]Institute of Adaptronic and Functional Integration, TU-Braunschweig, Langer Kamp 6, 38106 Braunschweig, Germany

Keywords: bonded repair, scarf joint, scarf repair, layer wise scarfing, composite repair

Abstract
Scarf repairs of aerospace composite structures are today's preferred technology. It is known that the shear stress distribution of the adhesive is inhomogeneous within the scarf. It depends on the stacking sequence and the scarf ratio. Main stress peaks are located at the interfaces of the 0 layers within the adhesive. A higher scarf ratio reduces these stress peaks at the cost of an increased joint size. A comprehensive study has been performed developing a methodology to reduce these shear stress peeks within state of the art composite scarf joints. The proposed method is a layer wise adaptation of the scarf ratio. Presented analytical calculations outline the concepts feasibility. An increased joint strength of layer wise scarfed coupons compared to constant ones is experimentally validated. Initial results show an increase in joint strength up to 50%. This improvement is a first step on the way towards size reduced composite repairs. The study's results are relevant to increase the number of bonded repairs under current certification restrictions and to develop high strength composite scarf joints.

1. Introduction

It is reasonable to assume that the number of repairs to composite structures will increase in the coming years due to the growing share of composites in civil aircrafts [1]. A damaged structured can be repaired by bonded or bolted repair [2]. Advantages of bonded scarf repairs are a high strength restoration, thermal and stiffness compatibility to the original laminate, flushness and a low visible profile. Main disadvantages are a high manufacturing complexity and lead time [3]. Incidents in the past regarding process safety lead to certification restrictions [4] which limits the applicability of bonded scarf repairs. Main consequence of regulation AC20-107B [5] is that bonded repairs are restricted to damage sizes below the structural limit load capability. The scarfed area is typically taken into account for the damage category assessment. Considering typical scarf ratios of SR 1:50 [6] even small damages can fall into higher damage classes limited to bolted repairs. Additionally large scarfs interfere with part edges and load introductions more often. Repair complexity and lead time increases accordingly. It is therefore desirable to reduce the size in order to repair larger damages by bonding or to avoid more complex scenarios.

2. Theoretical Analysis

According to Wang et al. [7] scarf joints show diverse failure modes categorized into laminate and adhesive failure. In order to restore the original strength of the parent laminate adherent failure prior to

Excerpt from ISBN 978-3-00-053387-7

the adhesive is desired. Several authors have shown that higher scarf ratios increase the joint strength and reduce shear stresses of the adhesive [8]. Adhesive shear stress varies along the bond line for composite adherents the. Equation 3 shows that the local shear stress is a function of the scarf angle and local ply stresses which itself depends on the ply stiffness [9]. Breitzmann et al. [10] tried to homogenize the shear stress distribution by adapting the local ply stiffness. This was achieved by numerically optimizing the patch stacking sequence. The calculated ply sequence lead to a nearly constant stress distribution demonstrating the theoretical feasibility of the concept. Unfortunately an experimental validation was not feasible. The optimized stacking was unbalanced and unsymmetrical. The presented work follows a second option offered by equation 3. Instead of adapting local stiffness a ply specific scarf angle is proposed. Figure 1 shows the balance of forces in a scarf joint. Equations 1-3 show that the adhesive shear and peel stresses solemnly depend on the scarf angle. A ply specific scarf angle is calculated by equation 5 depending on the adhesive shear strength $\tau_{adh,f}$, laminate failure strain $\epsilon_{lam,f}$, and local ply stiffness E_i. Assuming a typical stacking sequence of 0°, 90°, +45° and −45° plies three different scarf angles are calculated. This way the dominating adhesive shear stress at a 0° ply is much smaller compared to a constant scarf. The shear stress is reduced up to approximately 55% for a scarf ratio of SR 1:20 assuming a linear elastic material behaviour.

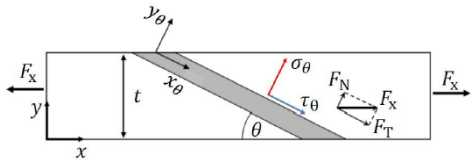

Figure 1. Balance of forces in a scarf joint

$$F_N = F_x \cdot \sin(\theta) \qquad \text{and} \qquad F_T = F_x \cdot \cos(\theta) \tag{1}$$

$$with \quad A_\theta = b \cdot \frac{t}{\sin(\theta)} = \frac{A}{\sin(\theta)} \tag{2}$$

$$\text{peel stress:} \quad \sigma_\theta = \frac{F_N}{A_\theta} = \sigma_x \cdot \cos^2(\theta) \qquad \text{shear stress:} \quad \tau_\theta = \frac{F_T}{A_\theta} = \frac{1}{2}\sigma_x \cdot \sin(2\theta) \tag{3}$$

$$\text{with Hook's law:} \quad \sigma_x = E_i \cdot \epsilon_{lam,f} \tag{4}$$

$$\theta_i = \frac{1}{2} \cdot \arcsin\left(\frac{2 \cdot \tau_{adh,f}}{E_i \cdot \epsilon_{lam,f}}\right) \tag{5}$$

3. Methods

The following work tries to validate an increase in joint strength compared to a constant scarf in tension loading. Reduced scarf ratios are investigated additionally demonstrating that variable scarf joints are capable of sustaining the same load compared to a constant scarf but with a shorter bond line.

3.1. Materials and Specimens

A specimen configuration similar to the AECMA prEN 6066 standard [11] is chosen to investigate constant and variable scarf joints. Figure 2 shows a sketch of the used specimen type. The chosen material for both parent and patch laminate is Hexcel Hexply 8552/33%/134/IM7(12K). Henkel EA9695 0.05psf NW epoxy film adhesive is used for bonding. A quasi-isotropic layup of $[45, 0, -45, 90, 45, 0, -45, 90, 45, 0, -45, 90]_s$ is investigated. The cured laminate has a thickness of about 3.1mm. The UD-ply data has been taken

Excerpt from ISBN 978-3-00-053387-7

from multiple sources and averaged ([12], [13], [14]). The adhesive's material shear strength of $\tau_{adh,f} = 51.4MPa$ has been determined with tube torsion specimen in an internal test campaign for a pure shear loading and is in line with data from the FAA [15]. The material input data is summarized in table 1.

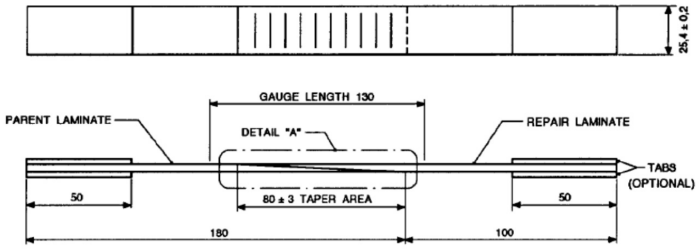

Figure 2. Tension specimen according to 6066 standard [11]

The optimum scarf angles taken from equation 5 are slightly adapted to the manufactured laminate thickness of 3.1mm. The scarf length of the corresponding constant and variable scarf now matches exactly but scarf ratio differs slightly. The increase in bonding area due to a variable scarf is only minor and does not impact joint strength.
Seven different sets of specimens are investigated. Two reference specimens are used to acquire adherent laminate strength and failure strain. This is a needed input for equation 5. Three corresponding sets of variable and constant scarf joints are tested for the global scarf ratios of SR 1:10, SR 1:20, and SR 1:30. The design data is summarized in table 2.

Table 1. Input data for analytical calculations

E_{11}	E_{22}	ν_{12}	G_{12}	t_{ply}	$\tau_{adh,f}$
MPa	MPa	1	MPa	mm	MPa
172.322	9291.0	0.32	5450.0	0.125	51.4

Table 2. Comparison of constant and varied angles for manufactured specimen (thickness = 3.1mm)

Specimen ID	Ref	C-1-10	V-1-10	C-1-20	V-1-20	C-1-30	V-1-30
Repetitions	2	4	4	4	4	4	4
Ply angle	none	$\theta_{const,1:10}$	$\theta_{var,1:10}$	$\theta_{const,1:20}$	$\theta_{var,1:20}$	$\theta_{const,1:30}$	$\theta_{var,1:30}$
[°]	-	[°]	[°]	[°]	[°]	[°]	[°]
0	-	5.89	2.43	2.95	1.21	1.97	0.81
±45	-	5.89	8.02	2.95	4.06	1.97	2.72
90	-	5.89	45.00	2.95	26.58	1.97	16.15
Length[mm]	-	30.01	29.99	60.07	60.00	90.01	90.00
Bond Length [mm]	-	30.17	30.44	60.15	60.24	90.06	90.15
Scarf Ratio	-	9.68	9.67	19.37	19.35	29.04	29.03

3.2. Manufacturing

All specimens are manufactured in a similar way. The UD-plies are cut on a numerical controlled cutter and stacked manually on a steel tool (figure 3a). The laminate is cured for 2h and 7bar absolute pressure

Excerpt from ISBN 978-3-00-053387-7

in an autoclave in accordance to the data sheet [16] at 180°C. The cured laminate is than cut in two parts. Both parts are machined on a numerical controlled milling machine. The constant and variable scarfs are milled with a PCD cutter at a feed rate of 800mm/min and a turn rate of 21.000 rpm. The scarf contour is controlled by photogrammetry and laser scanning afterwards. No significant deviation from the nominal contour has been found. All manufactured scarfs are cleaned with iso-propanol to remove grease and dried prior to bonding. Two scarfed plates are positioned and fixated by two 2mm steel pins (figure 3b). The film adhesive is cured for 2h at 3bar absolute pressure at 130°C. finally all specimens are cut by a diamond saw from the bonded plates to the proper size.

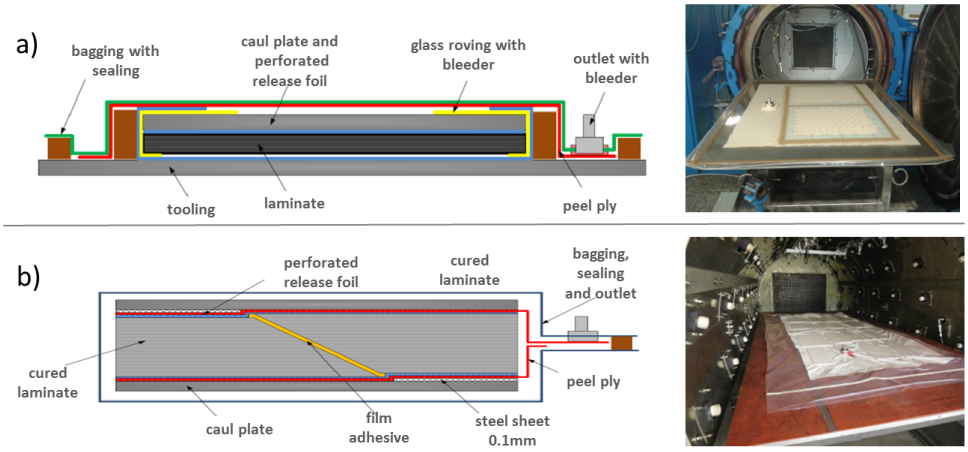

Figure 3. a) Laminate manufacturing, b) Bonding setup

3.3. Test Setup

All specimens are tested in pure tension mode. A Zwick 1448 testing machine with an internal 250kN load cell is used. At least one of each specimens is equipped with a strain gauge to acquire the Young's modulus and failure strain. The gauge is positioned outside the joint area. A GOM ARAMIS 12M system is used to measure the joint's deformation from side view. The system uses stereo optic digital image correlation (DIC) to measure the strain state. Figure 4 visualizes the test setup. All specimens need to be prepared with a suitable stochastic pattern. A special preparation procedure allows a resolution of $0.03mm^2$ which is sufficient for measuring the bond line deformation. The specimens are tested with hydraulic grips to minimize slippage.

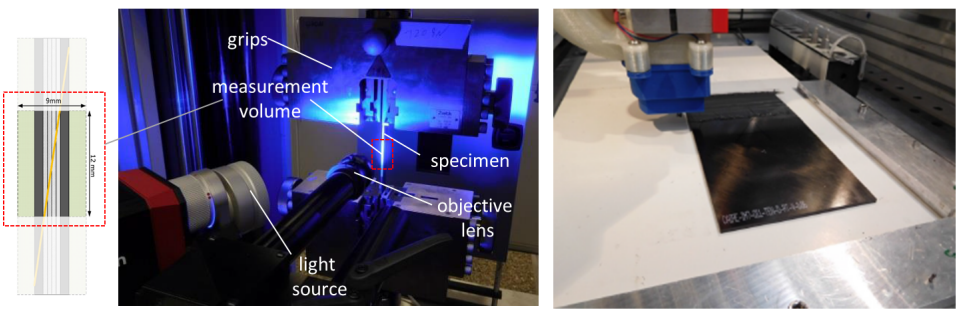

Figure 4. Test setup (left) and milling of scarf (right)

Excerpt from ISBN 978-3-00-053387-7

4. Results

All tests have been statistically evaluated by mean values and standard deviation. Failure Stress is given in percentage of the reference specimen. Table 3 summarizes the test results. Each groups mean of failure stresses is referenced to the original laminate strength. The constant scarf of SR 1:10 achieves approximately 40% of the original laminate strength, SR 1:20 about 46%, and SR 1:30 about 65%. The results are in line with other authors e.g. [8]. All variable scarf joints show a higher strength compared to the corresponding constant one. Statistical evaluation by 2-sample student t-test shows a significance for an increase of strength for the scarf ratio SR 1:10 (p=0.035) and SR 1:20 (p=0.001), but not for SR 1:30 (p=0.31). The variable V-1-20 specimen shows the biggest increase of about 50% compared to the constant scarf C-1-20. Microscopic investigation of the break surface shows a combination of cohesive adhesive failure and matrix failures within the 90° and 45° layers. A failure cascade cannot be derived from these results.

Table 3. Results from tests, failure stress in percent of the original strength

Specimen ID	Ref	C-1-10	V-1-10	C-1-20	V-1-20	C-1-30	V-1-30
Strength in [%]	100	40.62	47.2	46.37	70.46	64.58	67.24
Stdv.	0.7	3.1	0.7	2.3	4.9	3.5	0.9

The results from digital image correlation give a better insight into the joint's failure. Figure 5 shows some results taken from the constant SR 1:10 and variable SR 1:10 specimen. The constant specimen shows broad areas of increased tension strains which correlates with the ends of the 0° plies (figure 5 left). The constant and variable scarf shows matrix failure in the 90° layers prior to final failure (marked red). Delaminations grow steadily until final failure. The variable joint shows strain peaks as well. Closer evaluation reveals that these peaks are localized at the ends of the 90° layers. This is also supported by their small dimension. The 90° layers of the V-1-10 specimen have a 45° scarf angle which limits the run out to less than 1mm. These peak stresses can be found for most variable scarf joints.

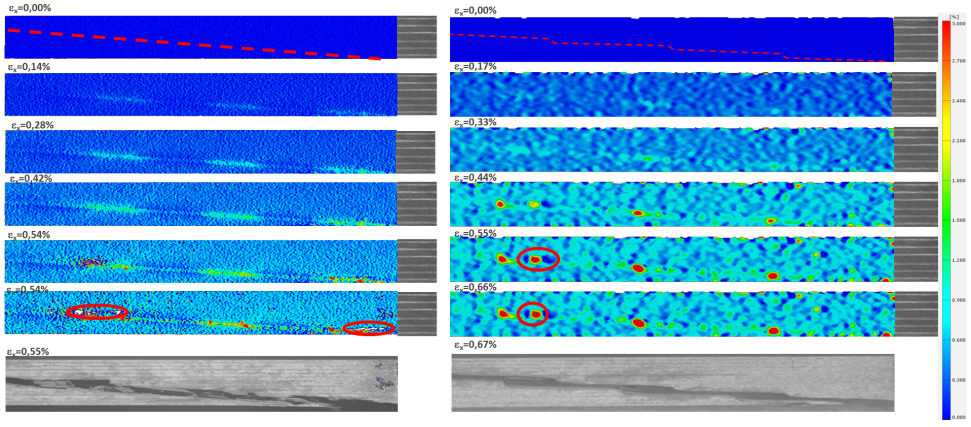

Figure 5. Strain measurement results: Tension strain ϵ_x for constant scarf ratio 1:10 (left) and variable scarf SR 1:10 (right)

Excerpt from ISBN 978-3-00-053387-7

5. Discussion

The variable V-1-10 scarf joint exceeds the constant C-1-20 joint despite its reduced bond line. The bonding surface of V-1-10 is only half of the constant scarf C-1-20. The variable V-1-20 scarf also exceeds the constant C-1-30 joint. The bonding surface of V-1-20 is only two thirds of C-1-30. This underlines the potential of repair size reduction by layer wise variable scarf joints. The variable V-1-30 scarf does not continue this line.
Figure 6 evaluates equations 3 and 4 for different laminate strains. It visualizes the results for constant SR 1:20 and variable SR 1:20 joints. The analytic model predicts an adhesive shear strength failure at the 0° ply interfaces for constant specimens. The shear stress exceeds the adhesive shear strength at a strain of 0.6%. The DIC and microscopic results support that failure mode. C-1-20 fails at 0.73%. One reason for the difference is that the analytic solution is based on a linear elastic material law of the adhesive. The analytic model overrates the shear stresses. Hence reduced failure strains are predicted. Variable joints show a different behaviour (figure 6). The adhesive shear stresses at the 0°, 45° and 90° interfaces are identical. The scarf angels are designed for an adhesive shear strength failure at laminate failure's strain (about 1.38%). The validation of the variable joint V-1-20 demonstrates a superior strength compared to C-1-20 but fails at 0.97% strain. The non linear material behaviour of the adhesive should further increase the failure strain. Instead it is smaller than expected.

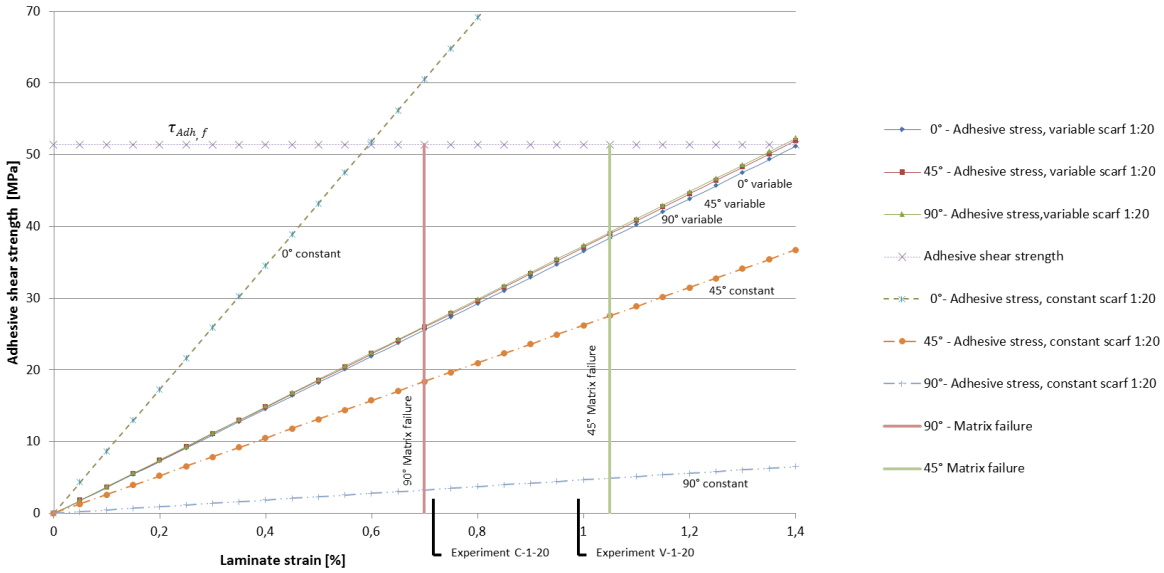

Figure 6. Analytic model of adhesive shear stresses (SR 1:20) for constant and variable scarf joints

A possible explanation is given by figure 7. Matrix failure has been integrated into the model. Load is shifted from degraded (90° and 45°) to the remaining 0° plies within the advanced model. Puck criterion is used to calculate the failure index. Classical laminate theory provides the proper failure strain. The prediction for the constant specimen C-1-20 does not change at all. It still predicts an adhesive shear strength failure. A shift of load from the 0° plies to the 45° and 90° would still result in an overloading of the adhesive. Failure prediction of the variable joint V-1-20 changes in the advanced model. As the adhesive stresses passes the 90° matrix failure strain, adhesive stress only increases in a small portion in the other plies. Stress increase is much bigger when the matrix degrades in 45° plies. The redistributed stress exceeds the adhesive shear strength at the 0° plies instantaneously. The adhesive fails due to shear strength failure but is originated in the matrix failure of the 45° plies. The DIC results support the assumption that extensive matrix failure of the 90° plies has occurred in the variable joints before final

Excerpt from ISBN 978-3-00-053387-7

failure. The improved model predicts the failure of variable joints of SR 1:20 much better. Joint failure of variable scarfs can be approximated by the matrix failure of the 45° plies. This approximation seems to be valid for the technical relevant scarf ratios of SR 1:10 up to SR 1:20. Table 4 summarizes the results of both models. Table 4 summarizes the analytical prediction for the tested specimen.

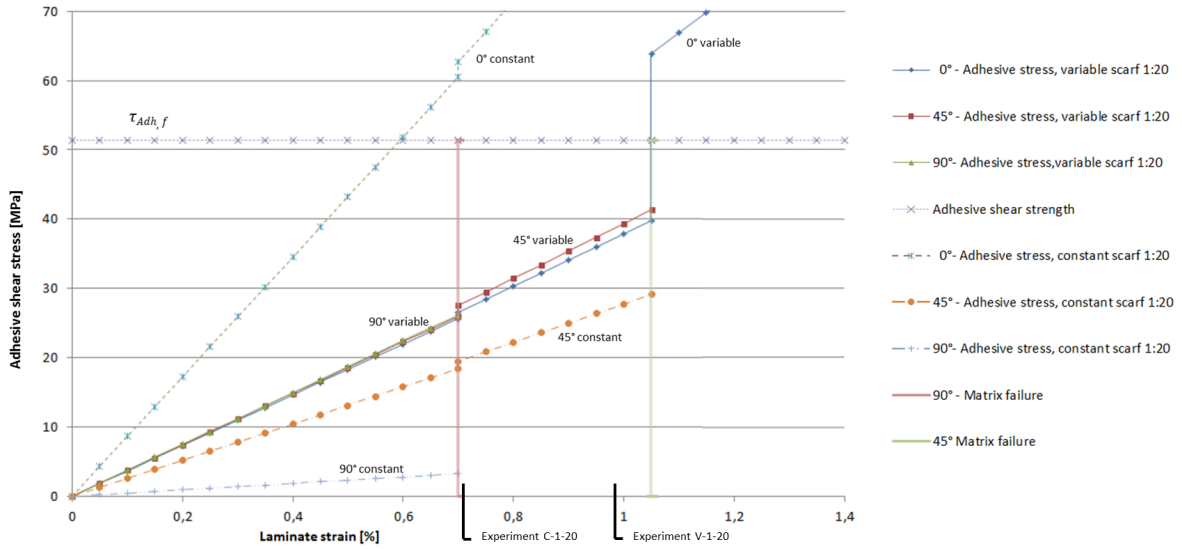

Figure 7. Analytic model of adhesive shear stresses (SR 1:20) for constant and variable scarf joints with influence of matrix degradation

Table 4. Experimental and predicted failure strains

ID	Experiment	Basic model without matrix failure	Deviation without matrix failure	Advanced model with matrix failure	Deviation with matrix failure
C-1-10	0.55	0.3	-45	0.3	-45
C-1-20	0.73	0.6	-18	0.6	-18
C-1-30	0.96	0.9	6	0.88	7
V-1-10	0.67	0.7	4	0.7	4
V-1-20	0.96	1.38	44	1.05	9
V-1-30	0.97	1.38	42	1.25	29

6. Summary and Outlook

The presented work demonstrates the potential of layer wise scarfed joints to reduce adhesive stresses and to improve joint strength. The experimental validation also shows that a size reduction of 30% - 50% is possible depending on the scarf ratio. The work uses a simple analytical foundation by Baker et al. [9] to pre-design the ply dependent scarf angles and validates different configurations in coupon tests. The basic analytical model under-predicts the failure strains of the constant specimen which is originated in the elastic plastic material behaviour. The prediction of variable joints overshoots instead. An advanced model incorporating matrix failure drastically improves precision and gives a reasonable explanation for the failure cascade. Final collapse of the variable scarf joints is an adhesive shear strength failure caused by matrix degradation in the 45° plies.

Excerpt from ISBN 978-3-00-053387-7

Future work is planned to validate the method of layer wise scarfing on more complex specimen like full 3D repairs. A numerical model will be developed to take the non linear material behaviour as well as more complex load scenarios into account.

References

[1] Christian Sauer. Lufthansa perspective on applications and field experiences for composite airframe structures. *3rd Commercial Aircraft Composite Repair Committee (CACRC) Meeting and Workshop for Composite Damage Tolerance & Maintenance*, 5.6.2009.

[2] K. B. Armstrong and R. T. Barrett. *Care and Repair of Advanced Composite Structures*. R: Society of Automotive Engineers. Society of Automotive Engineers, 1998.

[3] K. B. Katnam, L. F. M. Da Silva, and T. M. Young. Bonded repair of composite aircraft structures: A review of scientific challenges and opportunities. *Progress in Aerospace Sciences*, 61(0):26–42, 2013.

[4] Simon Waite. Easa perspective on safe maintenance practice: some regulatory concerns, 05.2007.

[5] FAA. *AC20-107B*. U.S. Department of Transportation, 2009.

[6] C. Soutis and F. Z. Hu. A 3-d failure analysis of scarf patch repaired cfrp plates. *American Institute of Aeronautics and Astronautics, Inc*, 1943:1971–1977, 1998.

[7] Chun Hui Wang and Cong N. Duong. *Bonded Joints and Repairs to Composite Airframe Structures*. Academic Press, 2015.

[8] Bonded repair of cfrp primary structure: Testing and analysis of bonded scarf joints, 24.-28. June 2012.

[9] A. A. Baker, Stuart Dutton, and Donald Kelly. *Composite materials for aircraft structures*. American Institute of Aeronautics and Astronautics, Reston and VA, 2 edition, 2004.

[10] T.D Breitzman, E.V Iarve, B.M Cook, G.A Schoeppner, and R.P Lipton. Optimization of a composite scarf repair patch under tensile loading. *Composites Part A: Applied Science and Manufacturing*, 40(12):1921–1930, 2009.

[11] AECMA Standard. Determination of tensile strength of a tapered and stepped joints, 1995.

[12] P. P. Camanho, P. Maimí, and C. G. Dávila. Prediction of size effects in notched laminates using continuum damage mechanics. *Composites Science and Technology*, 67(13):2715–2727, 2007.

[13] Kristin Marlett, Yeow Ng, and John Tomblin. Hexcel 8552 im7 unidirectional prepreg 190 gsm & 35% rc qualification material property data report. *National Center for Advanced Materials Performance, Wichita, Kansas. Test Report CAM-RP-2009-015, Rev. A*, pages 1–238, 2011.

[14] Yuri Nikishkov, Andrew Makeev, and Guillaume Seon. Progressive fatigue damage simulation method for composites. *International Journal of Fatigue*, 48:266–279, 2013.

[15] FAA. Shear stress-strain data for structural adhesives, 2002.

[16] Hexcel Composites. Hexply® 8552 epoxy matrix (180c/356f curing matrix) - product data, 2008.

Excerpt from ISBN 978-3-00-053387-7